Hyperspectral Imaging Technique to Analyse Fruit Quality using Deep Learning: Apple perspective

Manoj Chandak[1], Sunita Rawat[2]

Abstract: Apple is the world's most consumed fruit after banana. Bruising is one of the major causes of losses incurred by fruit and vegetable suppliers. This study aims to automate the identification of apple bruises using hyperspectral imaging [HIS] technology and the YOLOv5 algorithm, which is the latest convolutional neural network (CNN) model. Traditional methods of bruised apple detection with red-green-blue (RGB [Red-Green-Blue]) images are not very efficient, as color and texture may not be the dominant features for apple bruise identification. There are apple species such as Golden Delicious and Gala, which have dark red skin, and for those species, most RGB-based models give inaccurate results [1,5]. In the present study, honey-crisp and red-delicious apple species were scanned using a Resonon Pika NIR-320 hyperspectral imaging camera. The chemical characteristics of the scanned samples were analyzed in the laboratory. Lab-based chemical analysis results were used for testing and validation purposes. The two identified chemical properties used in this work are sugar content and O-H [oxygen-hydrogen] bonds. The results of this study will assist in establishing a standard bruise-detection system for industrial applications. The test results showed that the proposed detection model could recognize apple bruises with a mean average precision of 0.95 (mAP) and the classification accuracy of the validation system was found to be 96.22%.

Keywords: Hyperspectral Imaging; Pixel wise NIR spectra; Lasso regression; Naïve Bayes classification; YOLOv5; Bruise Detection

1. Introduction

Apple is a capitalistically important fruit with a wide variety of yields worldwide. In India, Apples are the third most valuable fruit, after mangoes and bananas. According to the latest information in recent years, apple production in India is approximately 2.3 million tonnes [1]. Owing to increasing demand, it is one of the most valuable crops both nationally and internationally and also has high industrial requirements.

In the process of bringing apples from farms to consumers, the major problem faced by the fruit and vegetables [1] industry is the loss due to bruising. At any stage of production, bruising can occur because of external forces, vibrations, or impacts. Bruising can also occur because of the harvesting, handling, transporting, and sorting processes. Consumers are thriving for fresh and perfectly shaped apples, and even minor imperfections are unacceptable.

There is a need for an effective system to distinguish affected samples at the early stages of the supply chain in order to separate them. Even slightly affected apples in the early stages may decay over time, emitting chemical gases. If these apples are not separated in time, they might affect the quality of other apples by emitting gases that are absorbed by the surrounding apples, initiating decay in healthy apples. Decayed apples are unacceptable to customers and do not meet the quality benchmarks of the international markets.

Most industries still rely on traditional manual methods for separating bruised apples from healthy apples. In most quality inspection sectors, the usual way for distinction is the workers' hands-on inspection of passing apples on conveyor belts and discarding bruised, damaged, and rotten apples. This process heavily depends on human senses, and with long working shifts, workers' efficiency reduces significantly, causing inconsistent segregation.

One important motive behind the present research is the development of a non-destructive methodology for bruise identification that can be easily realized for industrial utilization using hyperspectral imaging technology. The major challenges faced during the study of bruise detection are (a) multiple independent factors such as the cause of bruise, (b) impact severity, (c) apple species, and (d) harvest conditions that greatly affect accurate bruise detection.

2. Literature Survey:

(Mehl et al., 2004 Shahin et al., 2002) [2] and [3] used wavelength absorption for bruise detection. Studies were also conducted based on the duration of bruising. Apples with 1–30 days of bruising were scanned using X-ray imaging. The proposed method was not efficient for early and slight bruises on apples. The main contribution of the research work was:

(a) Classification of Bruised Apple's using Artificial Neural Network(CNN)

(b) Identification of NIR wavelengths, such as 685 nm, at which chlorophyll exhibits absorption, and other wavelengths, which shows the visual distinction between healthy and affected regions.

Further research by Kleynen et al. (2005) [4] clarified that early bruises and russet defects are still not segmented effectively

[1] *Shri Ramdeobaba College of Engineering and Management, Nagpur - INDIA*

[2] *Shri Ramdeobaba College of Engineering and Management Nagpur - INDIA*

* Corresponding Author Email: chandakmb@rknec.edu

because of color similarities with healthy tissues. The main contribution of research work was:

(a) The identification of the most impactful wavelength for bruised detection was found to be approximately 450, 750, and 800 nm. 2.450 nm wavelength effectively identified slight bruises. 3.750 nm and 800 nm wavelengths gave explicit distinction between healthy and affected tissues.

Systems developed until 2005 are still unable to provide an efficient solution for early bruise detection. Subsequent studies by Gamal et al. (2007) [5] focused on bruise detection by selecting three effective wavelengths in the NIR for detection. They relied on HSI [hyperspectral imaging] technology and targeted bruise detection on the sample after 60 min of impact.

Recent studies by Zhang and Li [6] (2018) used Hyperspectral Imaging and the AdaBoost algorithm. These studies showed that the average value of reflectance of the affected areas decreased with time since the time of impact. The 640–700 nm and 730–900 nm ranges showed prominent characteristics. The main contribution of research work was:

(a) Results concluded that the peak of absorption of sugar content was near 820nm.

(b) The valley in the spectral plot near the 960 nm wavelength reflects the 2nd harmonic of the O-H group in water. These studies aimed at reducing losses due to bruising by early detection of bruises and saving further losses on such fruit samples.

The proposed model in the research paper uses modern hyperspectral imaging technology and detection mechanisms [7] for bruise identification. For hyperspectral image acquisition, in the present research work, the near-infrared range [8] of (888.71 - 1714.63 nm) consisting of 168 bands was used.

In the year (2020), Gao et al. [9] researched strawberry ripeness. The spectral features identified for laboratory strawberries were two bands, specifically 528 nm and 715 nm, and those for field strawberries were 530 nm and 604 nm. These results are promising. The AlexNet CNN model was used for classification, and an accuracy of 98.6% was achieved.

Su et al. [10] (2021) contributed to fruit maturity classification by performing deep learning approaches and involving predictions of the soluble solid content in strawberries. They implemented one- and three-dimensional residual neural networks (RNNs). The main contribution of the research work was:

(a) Prediction of Soluble solids in strawberries using a deep-learning approach for fruit maturity classification.

(b) This study has provided the best utilization of hyperspectral data processed over deep neural networks for the implementation of a three-dimensional Residual Neural Network.

Torres-Rodriguez et al. [11] (2022, Q2) studied hyperspectral data and focused on the classification of sweet and bitter almonds using non-destructive methods for quality assurance. The spectral range used was 946.6 nm to 1648 nm. The main contribution of the research work was:

(a) Quality assurance and non-destructive methods for classification of sweet and bitter almonds using partial least squares discriminant analysis (PLS-DA) models.

(b) High Accuracy up to 99% without reduction of VIP scores for classification using partial least squares discriminant analysis (PLS-DA).

Hu et al. (2020) [12] focused on shape information for bruised apple detection. They used three-dimensional surface meshes obtained from a 3D Infrared Imaging System. They investigated (CNN) convolutional neural network (CNN) models with three different configurations and in association with transfer learning for the prediction of bruised apples. The main contributions of research work was:

(a) The proposed model successfully identified irregularities on the surfaces of bruised apples that are not commonly observed on unbruised apple surfaces.

(b) They were able to achieve a prediction accuracy of 97.67 from their best-configured model because transformations from (3D) surface meshes to (2D) feature maps were efficient.

Dhanashree Jawale et. al. (2017) [13] worked on techniques for the quick evaluation of fruits (apples). They classified apples based on size, shape, shading, and tissue. Image acquisition was performed using a thermal camera and modern image-processing methods. The proposed bruise detection system is composed of Image Acquisition, Preprocessing, Segmentation, Feature Extraction, Classification, and Comparison methods. The main contributions of research work was:

(a) Real-time detection with good speed and accuracy was made possible by the use of (an ANN) artificial neural network.

(b) Classification results using thermal camera images were much more reliable as compared to classification results obtained from web camera images.

Zhu et al. (2019) [14] used an SOC710-VP hyperspectral imaging system (with a wavelength range of 400–1000 nm) for image acquisition of 108 Fuji apples at five different intervals: 1 min, 1 d, 2 days, 3 days, and 4 days. Hyperspectral data smoothing and denoising were performed using the Standard Normal Variate (SNV) method. The main contributions of research work was:

(a) Apple bruise detection was performed using an Extreme Learning Machine (ELM), Partial Least Squares Linear Discriminant Analysis (PLS-DA), and Classification and Regression Tree (CART), among which 95.97% accuracy was achieved using the ELM model.

(b) The overall classification rate achieved using the Minimum Noise Fraction (MNF) was 92.90%.

Chiu et al. (2017) [15] developed an online apple bruise detection system. Impact forces of 67.9±4.84N, 82.1±4.57N, and 102±8.44N were applied on Golden Delicious apples to make bruises. The main contributions of research work was:

(a) They were able to detect bruises based on the fluorescence received from apple surfaces at a wavelength of 680± 10 nm. The fluorescence was captured using a color camera, and an excitation source with a 460 nm wavelength.

(b) Using the above-mentioned method, they achieved 100% accuracy for samples tested 45 min after impact.

Qi Pang et al. (2021) [16] used a long-wave near-infrared (LW-NIR 930–2,548 nm) hyperspectral imaging system to acquire

reflectance images of bruised apples. Three specific spectral regions and their characteristic wavelengths were identified using segmented principal component analysis of the regions of interest (ROIs). The main contributions of research work was:

(a) The results showed that the use of the YOLOv3 model with grayscale and principal component image datasets has great potential for the creation of bruise detection models.

(b) Using the grayscale dataset, all 110 bruised spots were identified, and the F1 score was 100%.

(c)The developed model also eliminated the misidentification of bright spots as bruised regions.

Beak (2019) [17] presented work on defect detection in a variety of apples using hyperspectral data spanning the visible (400 nm) to near-infrared (1000 nm). They selected five optimal bands using a sequential feature selection method over Apple's hyperspectral images. The selected bands were used for defect detection. The main contributions of research work was:

(a) A classification model was developed using a support vector machine (SVM). The accuracy of defect detection using SVM and SVM with Radial Basis Function (RBF) kernel was more than 90%.

(b) It was also found that the result of the SVM with the RBF kernel was more accurate than the Support Vector Machine (SVM).

Che (2018) [18] focused on pixel-based bruise region extraction using Vis-NIR Hyperspectral imaging. A 22-gram steel ball was released at an angle of 57 °hitting the apple at the equator, creating a bruise of approximately 1.4 cm in diameter. Data Size Compression and redundant data elimination were achieved using Principal component Analysis (PCA). The main contributions of research work was:

(a) SVM (Support Vector Machine) and RF (Random Forest) methods were applied for Bruised Region Extraction.

(b) The RF method (Random Forest) performed much better than the SVM with an average accuracy of 99.9 % %for bruise extraction.

Sakshi Goel (2019) [19] worked on Image Segmentation Algorithms for Detecting Defects on Fruit Surfaces. They detected defects in apples, such as fungal growth, bruising, and scab, using different image segmentation algorithms, such as the Gabor method, Clustering, Edge Detection, Otsu method, and watershed method. Yu Tang (2020) [20] graded apple bruises using Piecewise Nonlinear Curve fitting (PWCF) for Hyperspectral Imaging data. Pre-processing of Data was performed using Procrustes analysis (PA). The least-squares algorithm was used for PWCF to maintain the spectral information of the different patterns and reduce the dimensions of the spectra. The resulting spectral interval is connected to a low-dimensional feature descriptor. The main contributions of this paper are as follows:

(a) This model obtained the best grading accuracy of 97.33%.

(b).Reliable results were obtained using an error-correction output-coding-based support vector machine (ECOC-SVM) for bruise detection. For performance evaluation, the successive

projection algorithm (SPA), genetic algorithm (GA), principal component analysis (PCA), and kernel principal component analysis (KPCA) were used.

This research work is presented in various sections of this paper. Section I presents the introduction and related work. Section II describes the implemented methodology. Section III presents the results and discussion. Section IV presents conclusions and future work.

3. Methodology

3.1 Sample Preparation

Seventy-five apple samples were selected of which thirty-four were bruised and forty-one were not unbruised. The samples were scanned using a Pika-NIR 320 hyperspectral imaging camera. A standard procedure was followed to create the bruises. Bruises were introduced on equatorial surfaces by applying a force from the opposite sides to flat polished object surfaces.

The apples were scanned using a Hyperspectral Camera in sets. Each batch of apples was grouped into sets of four and positioned on the moving stage of the camera setup. Images from six different angles were captured: top, bottom, and four sides. To study the bruised regions after a certain duration of impact, samples were segregated in batches of 24 hours and 48 hours and kept at room temperature in a closed box. Furthermore, the accuracy of the statistical models was improved by selecting 189 more apple samples. Bruises were introduced to 136 samples as per the standard bruising procedure mentioned above. The remaining 53 samples were unbruised, except for the initially existing natural minor deformities.

3.2 Hyperspectral image acquisition system

The system used for the acquisition of hyperspectral images in a laboratory environment is Benchtop System reflectance. A Pika NIR-320 camera was mounted on the tower and the apple sample was placed on a linear moving stage below the camera, as shown in figure 1.

The Pika NIR-320 HIS Camera captured 168 spectral channels for each scanned image. The spectral resolution was 4.9 nm, and the images had 320 spatial channels. To achieve high accuracy, we consider bit depth =14 and calibration with white tile before the start of the sample scanning process. The camera has a maximum frame rate of 520, size (cm/in) of 11.0 x 29.6 x 8.9/4.3 x 11.7 x 3.5, and weight (kg/lb) 2.7 / 5.9. The setup had power requirements of 12V, 5A, and a pixel size of 30a. All 168 channels were in the NIR range of 888.71 - 1714.63 nm.

Figure:1: Benchtop Hyperspectral Imaging System

3.3 Spectral Extraction and datasets - Regression and classification model dataset preparation:

After the acquisition, the images were cropped, and a single hyperspectral image was created by combining images of four apples placed with a common face up. A CSV file of the dataset was then generated by cropping only the region specific to the apples, as shown in Figure 2. Further spatial mean data of 168 bands were generated using Spectronon software. The two datasets used for training the regression and classification models are described as follows.
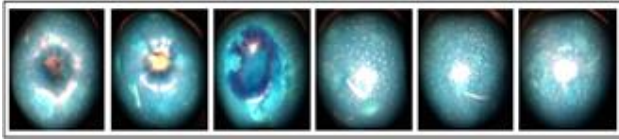
Figure:2: Scanned faces of a single apple

(a) The first type of analysis used 168 spatial mean values of the (apple-shaped) cropped region as independent variables and sugar content as the dependent variable.

(b) The second type of analysis used sugar as the independent variable and bruised and non-bruised spatial means as dependent variables (Table 1).

For the extraction of chemical properties and analysis of results, the samples were also analyzed in a Food Technology Lab. The samples scanned using the HSI camera were sent for analysis to the lab within 20 minutes of scanning. This helped to generate near-accurate results of the sugar content of the apples under consideration and to validate the object detector results. The first dataset was used for sugar prediction using regression analysis, while the second dataset was used to classify the apples (refer to Figure 3). The LASSO regression model [21] and Naive Bayes Classifier [22] were used to implement the above procedure.

Table 1: Spectral mean of spatial data and sugar content dataset

B1	B2	B3	B4	B5	….	B165	B166	B167	B168	Sugar content
2497	2535	2553	2560	2604	….	816	789	806	792	19.2
4055	4100	4141	4163	4214	…	1509	1477	1449	1454	17.97
1350	1389	1375	1373	1367	…	193	228	263	279	21.81
3221	3231	3268	3265	3279	…	1098	1092	1082	1112	19.59
4257	4307	4375	4342	4354	…	655	722	801	897	19.28
4500	4521	4554	4582	4557	….	1456	1503	1524	1590	17.85
……...	……...	……...	……...	……...	,...	……...	……...	……...	……...	……...
3415	3510	3523	3598	3597	...	1346	1298	1260	1255	18.37
4009	4053	4051	4114	4131	...	1669	1622	1582	1545	17.89
3640	3633	3648	3640	3656	...	440	468	513	573	19.78
4107	4130	4184	4197	4220	...	1922	1877	1819	1769	18
3410	3417	3418	3425	3465	...	477	488	514	567	19.87
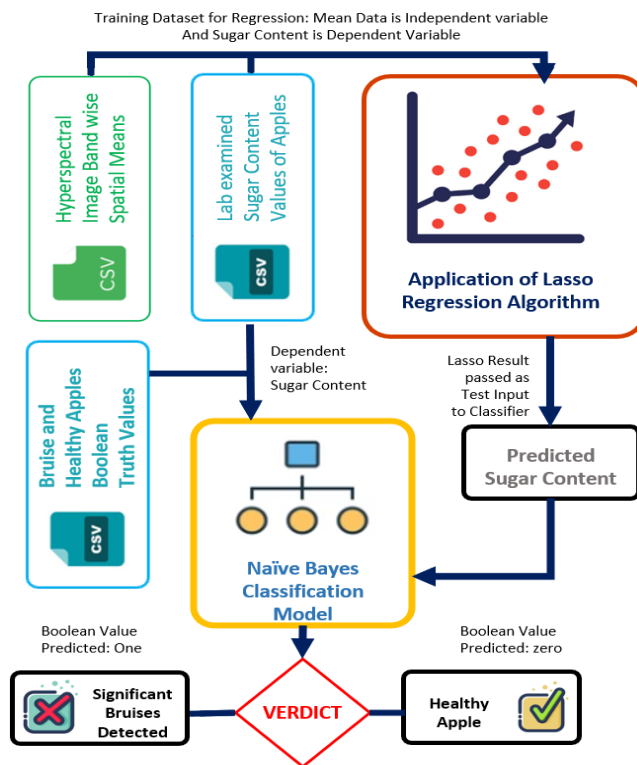
Figure 3: Process Flow for Regression and Classification

3.4 Object Detection Model Dataset preparation:

The research utilized the JPG image format for the bruise detection model. Three bands with prominent characteristics for bruised areas were selected from the scanned dataset of apple samples. It was determined that NIR bands near 960 nm were best suited for the research. Spatial mean data for the 956.51 nm, 961.36 nm, and 966.21 nm bands were generated for use in the study. To ensure compatibility with the object detector, reflectance values were normalized from 0-8000 to 0-255. This normalization improved the speed and accuracy of object detection. Additionally, the dataset images were augmented using rotation, width, and height shifts. The rotation range was set at 40°, and the width and height shift ranges were set at 0.2. Shear and zoom ranges were also set at 0.2. Horizontal and vertical flipping were enabled, and the fill mode was set to the nearest. JPG images were annotated for bruise detection using supervised learning. Labeling was necessary to provide object information for training the YOLOv5 model, and a labeling tool was used for this purpose.

3.5 Model Analysis and Automation Flow

1) Lasso regression

The Lasso regression is an improvement over linear regression because it incorporates the "L1 penalty," which regularizes the linear regression model. This penalty allows for automatic feature selection and identifies the coefficients of variables that do not significantly contribute to the prediction process. As a result, some variable coefficients are reduced to zero, simplifying the feature selection process and reducing the risk of overfitting. Lasso regression is a valuable tool for addressing overfitting..
The Lasso regression is expressed as:

$$Cost = RSS + \alpha * (|slope\ of\ best\text{-}fit\ line). \quad (1).$$

$$RSS = \Sigma\ (\ y - \hat{y})2\ . \quad (2).$$

Here,

y = mean spectral data of apple

ŷ = Best fit line between mean spectral data and sugar content

$$(L1)\ Penalty = \alpha * (|slope\ of\ the\ best\text{-}fit\ line) \quad (3).$$

Here, α (Alpha) helps compromise between the coefficient magnitude and balanced RSS values.

The value of α ranged from 0 to ∞. When α is 0, the equation becomes the same as that in the linear regression. When α is ∞,

all coefficients of the equation become zero, and the best-fit line becomes horizontal. When α is between 0 and ∞, it behaves normally. Lasso regression was applied to predict sugar content using the spectral band data of apples. A mean-squared error of 0.8589 was obtained after training the regression model.

2) Naïve Bayes classification

The Naive Bayes classification relies heavily on probability computation, as it is inspired by the Bayes Theorem. It is widely applicable in text classification of high-dimensional datasets. The use of precomputed and stored values of the input and output attribute classes improves the efficiency of the model. The algorithm also does not require epochs, iterations, or optimization, making it the fastest and simplest for classification tasks. In most classification algorithms, optimization requires a coefficient for the optimal result; however, no such coefficient is required in the Naive Bayes Classifier. [22].

$$Probability(A \mid X) = (Probability\ (X \mid A) \times Probability\ (A))/(Probability\ (X)\ ) \quad \cdots\cdots\cdots(4)$$

X is an attribute for a particular dataset (at1, at2, at3, …, atn) [in this case, sugar content].

ati = attribute of the dataset and

A = class of output attribute

3) YOLO v5 model

To identify bruises, the YOLOv5 model [24] and COCO (Common Object in COntext) dataset, a large-scale object detection and capturing dataset, are utilized. The COCO format is easily understood by neural networks. When choosing pre-trained models, various factors need to be taken into account, including personalized considerations related to an individual's research and objectives. Specifically, the YOLOv5s (Small) version was employed for training in this study. According to ultra-analytics, the YOLOv5s size is 14MB, with an inference speed of 2.2ms and mAP = 36.8, based on the PyTorch framework. It uses (.yaml) for configuration. YOLOv5s achieves the same accuracy as [16] compared to YOLOv3-416, with approximately ¼ of the computational complexity. The training was conducted using the pre-trained weights of YOLOv5s [25] and then trained on 438 images. Out of the 438 images, 350 were used for training and 88 for testing, representing an 80%-20% split of the available dataset.
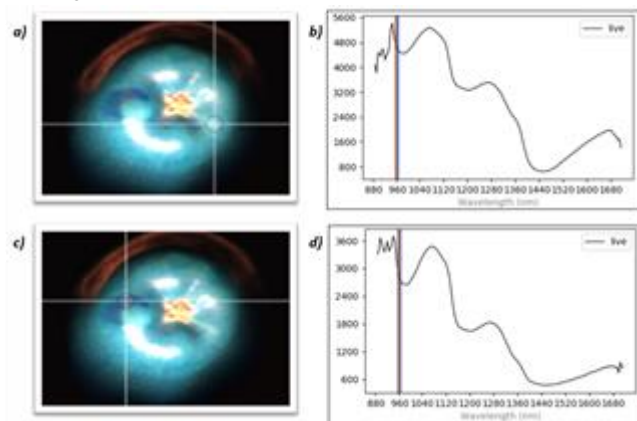
Figure 4: Reflectance vs. Wavelength Plot generated by Spectronon for AF-fromSelection.bil (+.hdr) a) at coordinates (54,55) and c) at coordinates (102,65). b) shows the plot for the non-bruised portion of the apple, the reflectance value of mentioned bands are higher for this pixel when compared to the d) plot for bruised region pixels having lower reflectance as seen in the plot

Even after performing preprocessing steps such as augmentation, resizing, and labeling, YOLO augments multiple training images in the specified larger image resolution and annotates modifications accordingly. This ensures accurate detection of slightly bruised areas and bruised areas near the corner of the apple section, as well as very small bruised areas. The outcome of object detection largely depends on the attribute values passed during training. The initial training was carried out with a low image size of 143 pixels, running for 150 epochs with a batch size of 32. This model was accurate for detecting large and prominent bruises but failed to detect smaller and slight bruises, as well as early bruised regions.

A second training run was carried out with the same batch size, but with an image size of 640 pixels, running for 150 epochs. Training on a larger image size made it possible to detect slight bruises, early bruises, and even bruises in very small regions. The result of this object detection is recorded in the annotation text file, which contains information on all detected bounding boxes.

3.6 Web Application

The application utilizes a hyperspectral image of the samples as its input. While the process is currently manual for demonstration purposes, it can easily be automated for industrial use. Automatic sample image passing can be implemented, and detection can be made continuous by feeding live video data of apples from the conveyor belts. The resulting hyperspectral images were processed, and spectral data with reflectance values were obtained. Three bands that have been previously observed in research were used to create bounding boxes for all detected bruised areas. The regression and classification models run automatically in the background to validate the results, which are then displayed. Bruised and non-bruised regions were successfully detected and validated. For a synopsis of the application part of the studies conducted in this study, please visit the video link: https://www.youtube.com/watch?v=zEfNIXmFHbo.

4. Results and Discussions

4.1 Band Selection and Chemical Analysis

In the 960 nm band, the absorption peak caused by the 2nd harmonic of the O-H group in water served as the basis for detecting bruises. Figure 4 displays the plot of reflectance versus wavelength. The first significant absorption valley near the 961.36 nm band, as well as the 956.51 nm and 966.21 nm surrounding bands, were selected for identifying bruised areas. The chosen image is submitted as a batch command to the system, and the bruise-detection model is run. The results are then presented on a web page. The boundaries between bruised and healthy tissues are clearly visible, as depicted in Figure 4, because the images do not have normal RGB pixel values, but rather encoded values of the reflectance data.

4.2 Object Detection Model Specifications

After preprocessing steps, such as augmentation, resizing, and labeling, the YOLO algorithm augments the training images to a larger image resolution. During training, the inference size (height, width) was set to (640, 640), with a confidence threshold of 0.25, an NMS IOU threshold of 0.45 for true positive detection, and a limit of 1000 maximum detections per image. This allows for accurate detection of slightly bruised areas and very small bruised areas. To better understand the results, the YOLOv5 losses and metrics are summarized in TABLE II. The key components of the YOLO loss function include box loss, obj loss, and cls loss (classification loss). Changes in mAP at an IoU threshold of 0.5 and the average mAP over the 0.5 to 0.95 range of IoU threshold values are also depicted in Table II.

TABLE II: YOLO TRAINING STATISTICS, SHOWING LOSSES, RECALL, PRECISION

Epoch	Train/BoxLoss	Train/ObjLoss	Metrics/ Precision	Metrics/ Recall	Metrics/ mAP-0.5	Metrics/ mAP-0.5:0.95	Val/ BoxLoss	Val/ ObjLoss
0	0.11023	0.031672	0.11132	0.021053	0.005468	0.002168	0.076596	0.076596
1	0.078688	0.026059	0.56166	0.094737	0.09063	0.01678	0.045773	0.045773
2	0.06518	0.023004	0.48436	0.17895	0.22335	0.056206	0.034454	0.034454
3	0.063891	0.021135	0.18222	0.094737	0.047794	0.013295	0.044893	0.044893
4	0.062206	0.017446	0.42125	0.45204	0.42528	0.099272	0.041123	0.041123
5	0.061139	0.018701	0.29383	0.36842	0.22771	0.043962	0.041992	0.041992
6	0.055511	0.017508	0.44375	0.43158	0.33579	0.075969	0.040113	0.040113
7	0.057873	0.017127	0.76768	0.63158	0.65112	0.2663	0.033933	0.033933
8	0.051209	0.017228	0.65644	0.54737	0.5363	0.1478	0.036023	0.036023
.....	.....	.....	.....	.....	.....	.....	.....	.....
28	0.034423	0.01295	0.88096	0.93684	0.94293	0.54262	0.020953	0.020953
29	0.038044	0.012592	0.81906	0.81005	0.85991	0.52371	0.021617	0.021617
30	0.033697	0.012818	0.76962	0.80879	0.82782	0.38481	0.029293	0.029293
31	0.034068	0.012617	0.90481	0.81053	0.92341	0.48329	0.024196	0.024196
32	0.036558	0.013148	0.93307	0.88421	0.9449	0.57692	0.020573	0.020573

4.3 Dataset Prerequisites and Restoring Dimensionality

Dimensionality reduction results in the loss of information, but the trade-off between speed and information loss is deemed acceptable after evaluating the results of the object detection process. The process leads to the loss of important unused band data, posing a challenge in restoring dimensionality to ensure accuracy in regression algorithms and making use of the feature selection property of the Lasso algorithm. To address this issue, the model designed maps the bruised area detected by YOLOv5 back to the raster file format, which is then read as a 3-D array. This generates two-dimensional data with 168 columns and several rows depending on the bruised areas detected by YOLOv5. Each value in the 2D data represents the spatial mean of the reflectance values of the detected bruised areas.

4.4 Results of Regression and Classification Algorithms

The LASSO regression algorithm was utilized to perform sugar prediction, resulting in a reduction of overfitting and improved output compared to linear regression. The mean square error of the Lasso regressor was 0.8589, with an alpha value of 5. Lasso regression outperformed other regression methods such as Random Forest and decision tree, which had mean squared errors (MSE) of 3.2803 and 3.3479, respectively. Additionally, the 48 most dominant wavelengths listed in TABLE III were extracted. A distribution plot, combining Kernel Density Estimation (KDE) and histogram, is depicted in Figure 5, demonstrating the variance in the data distribution. The plot indicates that maximum density is achieved when the variance in sugar is zero, showcasing the performance of the regressor. The predicted range of sugar in the testing dataset was between 16.3 – 23.5. Chemical property analysis revealed an inverse relation of magnitude between the sugar and reflectance spatial means of the bruise region. Furthermore, absorption peaks for bruised regions were observed at 820 nm and 960 nm for the sugar and second harmonic of O-H in water, respectively [23]. E. Final classification steps

The regression prediction step is cascaded using the Naïve Bayes classification algorithm. One important reason for using this classifier is its ability to perform probability calculations much faster than Logistic Regression or another tree-based algorithm. This helped classify the bruise and non-bruise regions with sugar value as the independent variable in one of the most efficient possible ways. In addition, the detection from YOLOv5 was validated. The last calibration step involved the use of a threshold value.

The ratio of non-conflicting results to the total results is calculated, and a low threshold of 30% is maintained to minimize False Positive proclaims [26]. This concludes with the contribution of the features and prediction of the sugar content. The value of sugar content is given to the Naïve Bayes classifier, which classifies whether the apple is bruised or not. This is a comprehensive description of the procedures and methods used throughout the study.
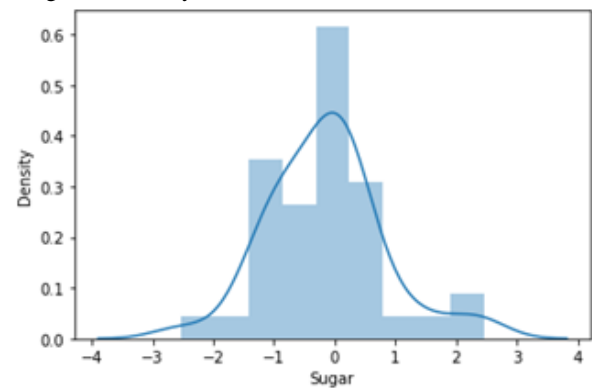
Figure 5: Sugar vs Density Chart

TABLE III: MOST CONTRIBUTING BAND FOR SUGAR PREDICTION IDENTIFIED BY LASSO

Band	Wavelength (nm)	Band	Wavelength (nm)	Band	Wavelength (nm)	Band	Wavelength (nm)
1	888.71	26	1009.96	38	1068.45	71	1230.32
2	893.55	27	1014.82	39	1073.34	72	1235.25
4	903.22	28	1019.69	53	1141.85	73	1240.18
6	912.9	29	1024.56	54	1146.75	75	1250.04
12	941.96	30	1029.43	57	1161.47	76	1254.97
13	946.81	31	1034.31	58	1166.38	78	1264.85
14	951.66	32	1039.18	59	1171.29	81	1279.66
16	961.36	33	1044.06	60	1176.2	107	1408.58
17	966.21	34	1048.93	62	1186.03	158	1664.12
23	995.36	35	1053.81	68	1215.54	159	1669.16
24	1000.23	36	1058.69	69	1220.47	160	1674.21
25	1005.09	37	1063.57	70	1225.39	168	1714.63

Figure 6 depicts the confusion matrix, summarizing the performance of Naïve Bayes classification algorithms. The following two images, Figure 7 and Figure 8, represent the comparison of the labeled bounding boxes and detected bounding boxes. The developed model is capable of detecting most types of bruises, achieving a mean average precision value of 0.95 after custom object training of the YOLOv5 pretrained model.

Figure 9 depicts the system flow, beginning with the input of the HSI image. The HSI image is initially converted to jpg using Python PIL's transformation functions. YOLOv5 is then utilized to analyze the transformed image, providing bounding box coordinates for bruised regions and generating an annotated image. Subsequently, the bruised detection validation process functions are invoked to obtain spectral data mapped to the

bruised region. These spectral data are then transformed into 2-D data with 168 channel values, each representing the spatial mean of the reflectance values for that channel. The data is input into lasso regression, which identifies the most influential features

and predicts the sugar content. The sugar content value is then passed to the Naive Bayes classifier, which determines whether the apple is bruised or non-bruised.
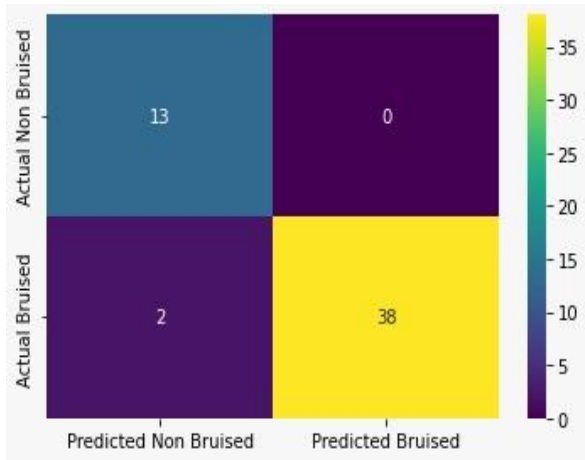
Figure 6: Confusion Matrix for Classification of Apple
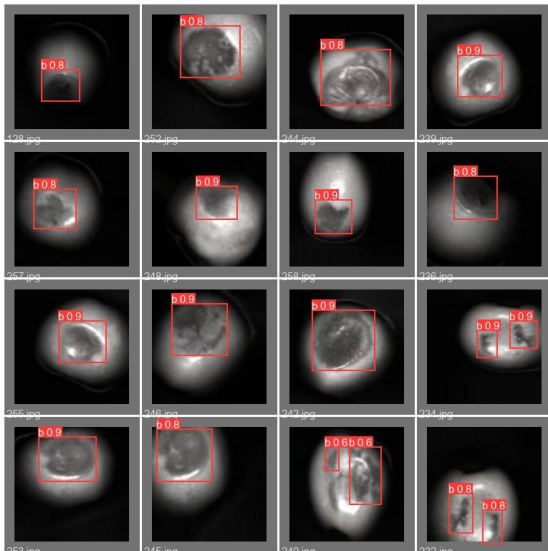
Figure 7: Autogenerated results after YOLO5 training
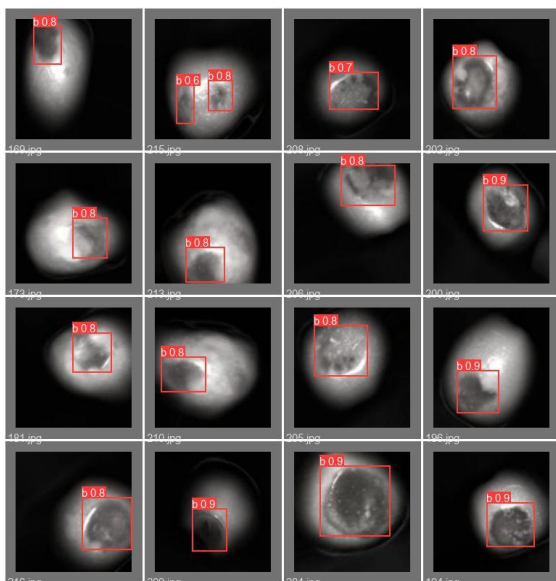
Figure 8: Autogenerated results after YOLO5 training
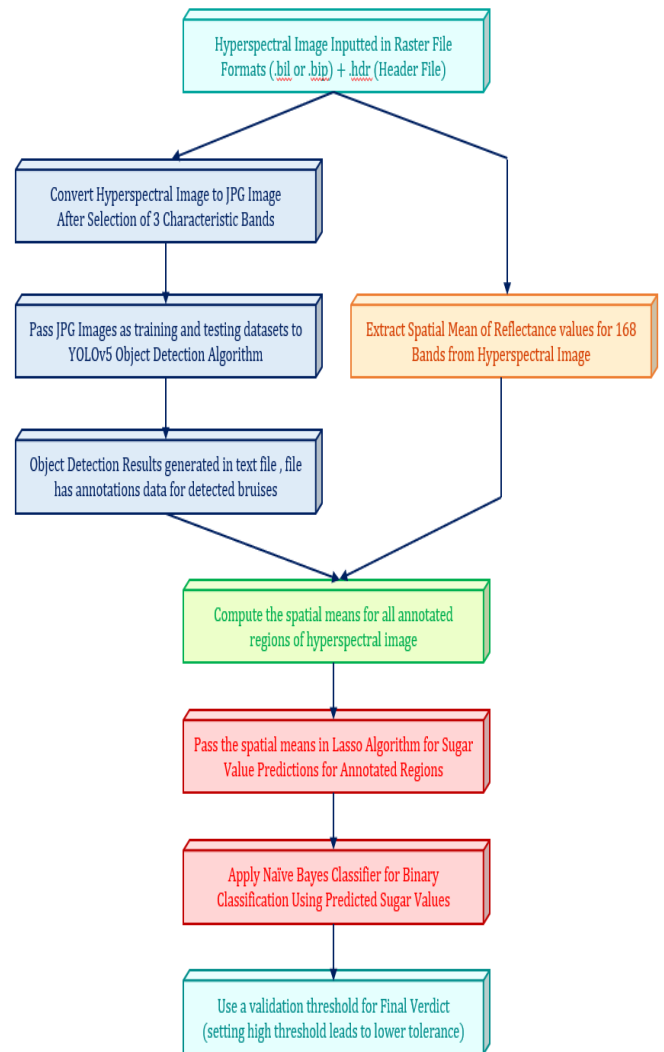
Figure:9: Brief Description of Process Flow

5. CONCLUSION

Our contribution to this field of study is the implementation of a validation system based on chemical analysis of samples for bruise detection. Previous research in [12], [13], and [14] has focused on detection mechanisms but has not addressed the issue of false positives. For example, [12] utilized 3D infrared imaging for bruise detection on apple surfaces, while [13] relied on size, shape, shading, and tissue characteristics. However, these methods were found to be less reliable and did not account for slight or early bruises. Similarly, [14] used hyperspectral imaging but did not incorporate chemical analysis-based validation procedures.

The presented study utilized NIR spectra stored pixel-wise in raster formats to detect a variety of bruises on apples, providing a more accurate dataset compared to traditional methods. We found that using spectral data in pixel-wise formats from the HSI for bruise detection of apple fruit was practical and reasonable. We also implemented YOLOv5 for object detection, which proved to be an important model for data analysis in this field.

One of the major challenges faced was detecting very slight bruises with minimal characteristic differences, as well as accounting for the wide variety of causes for bruising. However, the combination of algorithms used in our study significantly improved the detection results.

Two key components that contributed to our results were the use of higher wavelength near-infrared bands and the incorporation of chemical analysis of samples under image acquisition. We collected data from apples from a common regional yield, but believe that collecting apples from different orchard farms in various regions would significantly improve our results. In our study, the proposed detection model was able to recognize apple bruises with a mean average precision of 0.95 (mAP) and a validation system accuracy of 96.22%. We believe that increasing the dataset size will further improve the accuracy of our model.

REFERENCES

[1] Professor Da-Wen Sun , "Hyperspectral Imaging for Food Quality Analysis and Control", Food Refrigeration and Computerized Food Technology, National University of Ireland, Dublin (University College Dublin) , 2010

[2]. Mehl, P. M., Chen, Y. R., Kim, M. S., & Chan, D. E. "Development of hyperspectral imaging techniques for the detection of apple surface defects and contaminations." Journal of Food Engineering, 61(1), 67–81 , 2004 .[Crossref]

[3]. Shahin, M. A., Tollner, E. W., McClendon, R. W., & Arabnia, H. R. "Apple classification based on surface bruises using image processing and neural networks" Transactions of the ASAE, 45(5), 1619–1627, 2002. [Crossref]

[4]. Kleynen, O., Leemans, V., & Destain, M. F. "Development of a multispectral vision system for the detection of defects on apples." Journal of Food Engineering, 69(1), 41–49 , 2005 .[Crossref]

[5]. LEI FENG, SUSU ZHU, LEI ZHOU, YIYING ZHAO, YIDAN BAO, CHU ZHANG , AND YONG HE "Detection of Subtle Bruises on Winter Jujube Using Hyperspectral Imaging With Pixel-Wise Deep Learning Method " College of Biosystems Engineering and Food Science, Zhejiang University, Hangzhou 310058, China Key Laboratory of Spectroscopy Sensing, Ministry of Agriculture and Rural Affairs, Hangzhou 310058, China , May 16, 2019 [Crossref]

[6]. Meng Zhang & Guanghui Li "Visual detection of apple bruises using AdaBoost algorithm and hyperspectral imaging", International Journal of Food Properties, 21:1, 1598-1607, DOI: 10.1080/10942912.2018.1503299 , 2018[Crossref]

[7] Abbott, J. A., Lu, R., Upchurch, B. L., & Stroshine, R. L. "Technologies for non-destructive quality evaluation of fruits and vegetables", Horticultural Review, 20, 1–120, 1997

[8]. Wenqian Huangab, Baihai Zhang, Jiangbo Lib, Chi Zhang,Early "Detection of Bruises on Apples Using Near-infrared Hyperspectral Image" , School of Automation, Beijing Institute of Technology, No.5 Zhongguancun South Street, Beijing, China 100081; Dept. of Intelligent Detection, National Engineering Research Center of

Intelligent Equipment for Agriculture, No.11 Shuguang Garden Middle Road, Beijing, China 100097, 2013[Crossref]

[9] Zongmei Gao, Yuanyuan Shao, Guantao Xuan, Yongxian Wang,Yi Liu, Xiang Han "Real-time hyperspectral imaging for the in-field estimation of strawberry ripeness with deep learning", Center for Precision and Automated Agricultural Systems, Department of Biological Systems Engineering, Washington State University, Prosser, WA 99350, USA ,College of Mechanical and Electrical Engineering, Shandong Agricultural University, Tai'an 271018, China, Nanjing Institute of Agricultural Mechanization, Ministry of Agriculture and Rural Affairs, Nanjing 210014, China, College of Agriculture, Food and Natural Resources, University of Missouri, Columbia, MO 65211, USA , 27 April 2020.[Crossref]

[10] Zhenzhu Su, Chu Zhang , Tianying Yan, Jianan Zhu, Yulan Zeng, Xuanjun Lu, Pan Gao, Lei Feng, Linhai He, Lihui Fan ," Application of Hyperspectral Imaging for Maturity and Soluble Solids Content Determination of Strawberry With Deep Learning Approaches" , Institute of Biotechnology, Zhejiang University, Hangzhou, China, School of Information Engineering, Huzhou University, Huzhou, China, College of Information Science and Technology, Shihezi University, Shihezi, China, Key Laboratory of Oasis Ecology Agriculture, Shihezi University, Shihezi, China, College of Biosystems Engineering and Food Science, Zhejiang University, Hangzhou, China, Key Laboratory of Spectroscopy Sensing, Ministry of Agriculture and Rural Affairs, Hangzhou, China, Hangzhou Liangzhu Linhai Vegetable and Fruit Professional Cooperative, Hangzhou, China. 10 September 2021[Crossref]

[11] Irina Torres-Rodríguez , María-Teresa Sánchez , José-Antonio Entrenas , Miguel Vega-Castellote , Ana Garrido-Varo and Dolores Pérez-Marín "Hyperspectral Imaging for the Detection of Bitter Almonds in Sweet Almond Batches", Department of Animal Production, University of Cordoba, Rabanales Campus, 14071 Córdoba, Spain. Department of Bromatology and Food Technology, University of Cordoba, Campus of Rabanales, 14071 Córdoba, Spain. 9 May 2022[Crossref]

[12] Hu, Z., Tang, J., Zhang, P. and Jiang, J., 2020. Deep learning for the identification of bruised apples by fusing 3D deep features for apple grading systems. Mechanical Systems and Signal Processing, 145, p.106922.[Crossref]

[13] Jawale, D. and Deshmukh, M., 2017, April. Real time automatic bruise detection in (Apple) fruits using thermal camera. In 2017 International Conference on Communication and Signal Processing (ICCSP) (pp. 1080-1085).[Crossref]

[14] Zhu, X. and Li, G., 2019. Rapid detection and visualization of slight bruise on apples using hyperspectral imaging. International journal of food properties, 22(1), pp.1709-1719[Crossref]

[15] Yi-Chich Chu and Chun-Hung Chen "Development of an on-line apple bruised detection System" March 2017[Crossref]

[16] Qi Pang,Wenqian Huang,Shuxiang Fan,Quan Zhou,Zheli Wang,Xi Tian "DETECTION OF EARLY BRUISES ON APPLES USING HYPERSPECTRAL IMAGING

COMBINING WITH YOLOV3 DEEP LEARNING ALGORITHM" , 2021[Crossref]

[17] I. Baek, C. Eggleton, S. Gadsden, M. Kim"Selection of optimal band for developing multispectral system inspecting apples for defects". 30 April ,2019.[Crossref]

[18] Wenkai Che, Laijun Sun, Q. Zhang, Wenyi Tan, Dandan Ye, Dan Zhang, Yangyang Liu " Pixel based bruise region extraction of apple using Vis-NIR hyperspectral imaging" Key Laboratory of Electronics Engineering, College of Heilongjiang Province, Heilongjiang University, Harbin 150080, China, 14 January.[Crossref]

[19] Sakshi Goel , Mohit Kumar , Yogesh "An Improved Segmentation Algorithm for Detecting Defects on Fruit Surface" Amity University Uttar Pradesh, Noida, India ,2019[Crossref]

[20] YU TANG 1,2, SHENGJIE GAO1 , JIAJUN ZHUANG1 , CHAOJUN HOU1 , (Member, IEEE), YONG HE3 , (Member, IEEE), XUAN CHU1 , AIMIN MIAO1 , AND SHAOMING LUO2 "Apple Bruise Grading Using Piecewise Nonlinear Curve Fitting for Hyperspectral Imaging Data" 4 August ,2020.

[21]. Sunghoon Kwon, Sangmi Han, Sangin Lee "A small review and further studies on the LASSO". Department of Applied Statistics, Konkuk University Department of Statistics, Seoul National University Received, 2013. [Crossref]

[22]. Dr. Irina Rish,"An Empirical Study of the Naïve Bayes Classifier" , T.J. Watson Research Center, January 2001. [Crossref]

[23]. Kim, M. S., Chen, Y. R., & Mehl, P. M. . "Hyperspectral reflectance and fluorescence imaging system for food quality and safety", 2001. [Crossref]

[24]. Xingkui Zhu, Shuchang Lyu, Xu Wang, Qi Zhao "TPH-YOLOv5: Improved YOLOv5 Based on Transformer Prediction Head for Object Detection on Drone-captured Scenarios",26 Aug 2021[Crossref]

[25]. Peiyuan Jiang, Daji Ergu*, Fangyao Liu, Ying Cai, Bo Ma "A Review of Yolo Algorithm Developments" Key Laboratory of Electronic and Information Engineering (Southwest Minzu University),2022 [Crossref]

[26]. Xiaolin Zhu & Guanghui Li "Rapid detection and visualization of slight bruise on apples using hyperspectral imaging",13 Sep 2019. [Crossref].

PROF. Manoj Chandak is Dean of Academics and Professor in the Department of Computer Science and Engineering at Shri Ramdeobaba College of Engineering and Management, Nagpur. India. He has total of 27 years of academic experience. His areas of interest is Natural Language Processing, Machine Learning, Big Data Analytics, Cloud storage, and data management. He is also a recognized Ph.D. supervisor. His current research work includes the "**Development of coal quality exploration technique based on convolutional neural networks and hyperspectral images**". The project is completed in the stipulated time period, sponsored by the Ministry of Coal, Government of India with a grant of INR 1.03cr. He is also the principal investigator of the project entitled "Indigenous Development of NIR spectroscope for instant prediction of coal quality parameter, with a grant of 1.10Cr from the Ministry of Coal, Government of India.

Prof Sunita Rawat, is an Assistant Professor in the Department of Computer Science and Engineering at Shri Randeobaba College of Engineering and Management, Nagpur. She completed her Ph.D. degree with Machine Learning and Natural Language Processing as specializations. Her research interests include image processing, machine learning, and Artificial Intelligence. She is a member coordinator of the project entitled "Indigenous Development of NIR spectroscope for instant prediction of coal quality parameter, with grant of 1.10Cr from Ministry of Coal, Government of India.